JOURNAL OF APPLIED POLYMER SCIENCE VOL. 15, PP. 571–588 (1971)

Gel Permeation Chromatography: Physical Characterization and Chromatographic Properties of Corning Porous Glasses*

A. R. COOPER,† A. R. BRUZZONE, J. H. CAIN, and E. M. BARRALL II,**
Chevron Research Company, Richmond, California 95114

Synopsis

Five porous glasses, manufactured by Corning, reputed to have very narrow pore size distributions, have been characterized by mercury porosimetry, nitrogen adsorption–desorption isotherms, and electron microscopy. The characteristics of these glasses as packing materials in gel permeation chromatography have been determined. Using polystyrene solutes and toluene solvent at room temperature, the glasses in series combination of columns are capable of separating molecular weights from a few thousand to several million. These glasses are compared with other available materials for column packings in gel permeation chromatography.

INTRODUCTION

Porous glass column packings for use in gel permeation chromatography (GPC) are available, having a variety of pore sizes and pore uniformities. Previous publications have documented the GPC characteristics of a porous glass with an extremely wide pore size distribution[1] and glasses of various pore sizes with narrower pore size distributions.[2] Haller[3] prepared porous glasses of varying pore sizes with extremely narrow pore size distributions. These materials were used by Haller[4] to separate viruses and by Moore and Arrington[5] for the separation of polystyrenes and polyisobutenes. Recently, a commercial material manufactured by Corning (distributed by Waters Associates, Framingham, Massachusetts), possessing narrow pore size distributions similar to Haller's materials, became commercially available. This study involves the Corning Glass lot available in January 1970. Naturally, some variations will exist between various lots of material made by a batch process.

* Part I of a series on Characterization and Properties of Macromolecules.

† Present address: Department of Pure and Applied Chemistry, Thomas Graham Building, University of Strathclyde, Glasgow, Scotland.

** Present address: International Business Machines Corporation, Research Laboratory, Monterey & Cottle Roads, San Jose, California 95115.

EXPERIMENTAL

Mercury Porosimetry

A Micromeritics mercury porosimeter with a maximum operating pressure of 50,000 psi was used to characterize the porous glass samples. The results were calculated assuming a cylindrical pore model, a contact angle of 130 degrees, and the surface tension of mercury, 473 dynes/cm.

Nitrogen Adsorption–Desorption Isotherms

For the glasses having pore radii below 500 Å, the surface areas were determined by a BET analysis of the adsorption isotherm, and a pore size distribution was determined, assuming a cylindrical pore model, from the desorption isotherm. The liquid nitrogen micropore volume (that volume of pores having pore radii less than 500 Å) was also determined. For the glasses having pore radii larger than 500 Å, only the surface areas were determined.

Electron Microscopy

A well-mixed 0.3-g portion of the crushed glass having particle sizes 120–200 mesh was mixed with an epoxy-mounting resin prepolymer as described previously.[6] The impregnated samples were cast into the shape required by the Ultratome II ultramicrotome. Numerous sections were cut and floated on to carbon-coated electron microscope grids. Those sections thinner than 1000 Å (by interference color) were chosen for observation. The samples and grids were coated with carbon in a vacuum sputtering apparatus.

No replication or shadowing was required, as the electron contrast between the glass and the resin mounting was satisfactory for direct observation. The carbon coating was required to avoid the beam-induced sample charge. A Japan Electron Optics JEM 6-A electron microscope operated at 80 kV was used to examine the samples. The micrographs were made on Kodak medium projector slide glass plates developed in Kodak HRP high-resolution developer. The magnification of the microscope at 80 kV was calibrated by the standard diffraction grating technique.

Gel Permeation Chromatography

The five available porous glasses, having particle sizes in the 120–200 mesh range, were packed as dry materials into stainless steel columns 4 ft in length and 0.305 in. internal diameter. After packing, the columns were pumped with toluene for 24 hr and then installed in the gel permeation chromatograph. Narrow molecular weight distribution polystyrene standards (Pressure Chemical Company, Pittsburgh, Pennsylvania) were used to characterize the elution volume molecular weight relationship of each of the five columns. The polystyrenes were injected as 0.1 wt-% solutions in toluene using an injection loop of volume 1.77 ml and a flow rate of 1 ml/min.

RESULTS AND DISCUSSION

The results of the physical characterization of Corning porous glasses are shown in Table I. The pore radii and pore volume distributions from electron microscopy, mercury porosimetry, and nitrogen adsorption–desorption isotherms are compared with the manufacturer's quoted values.

Electron Microscopy

CPG 10-2000 (Fig. 1). This glass is characterized by very regular pore diameters and very few large voids. In the three fields examined, there was no evidence of very small pores. The average diameter of 150 pores measured was 2030 Å. The distribution around the mean was narrower than that previously obtained for Bio-Glas samples furnished by Bio-Rad Laboratories. This sample truly resembles the material reported by Haller.[3] The glass wall thickness is minimized in this sample. Seventy-five per cent of the total fields measured consisted of open pores. This is a very large active volume for a porous glass material—on the basis of previous experience.

Fig. 1. Electron micrographs of porous glass CPG 10-2000. Magnification 40,000×.

TABLE I
Pore Radii and Pore Volume Distributions of Corning Porous Glasses

Sample designation	Manufacturer's values pore radius, Å	Electron microscopy average pore radius, Å	Mercury porosimeter pore radius, Å			Nitrogen adsorption–desorption isotherms pore radius, Å		
			At maximum in differential pore volume distribution	At base of differential pore volume distribution[a]		Average pore radius, Å	At maximum in differential pore volume distribution	At base of differential pore volume distribution[a]
CPG 10-240 Lot. No. 8282P	137 ± 12.1%	See Text	168	218 (4%)	126 (98.5%)	271[b] 283[c]	200	220 (1%) 125 (95%)
CPG 10-370 Lot No. 8261P	185 ± 8.1%	See Text	224	282 (1.0%)	180 (96%)	313[b] 320[c]	270	300 (5%) 180 (95%)
CPG 10-700 Lot No. 8264S	395 ± 14%	375	474 474	632 (0.5%) 596 (1.5%)	376 (93.0%) 355 (95%)	820[c]		
CPG 10-1250 Lot. No. 8255	700 ± 13.5%	550	751 751	1001 (0.5%) 1001 (0.5%)	596 (95%) 563 (93%)	1613[c]		
CPG 10-2000 Lot No. 8154	1150 ± 8.5%	1015	1335	1781 (0.5%)	1061 (91%)	2411[c]		

[a] The values in parentheses indicate the percentage integral pore volume at which the quoted radii occur.

[b] Calculated from $\frac{2 \times \text{liquid nitrogen micropore volume}}{\text{BET surface area}}$.

[c] Calculated from $\frac{2 \times \text{mercury pore volume}}{\text{BET surface area}}$.

(2)

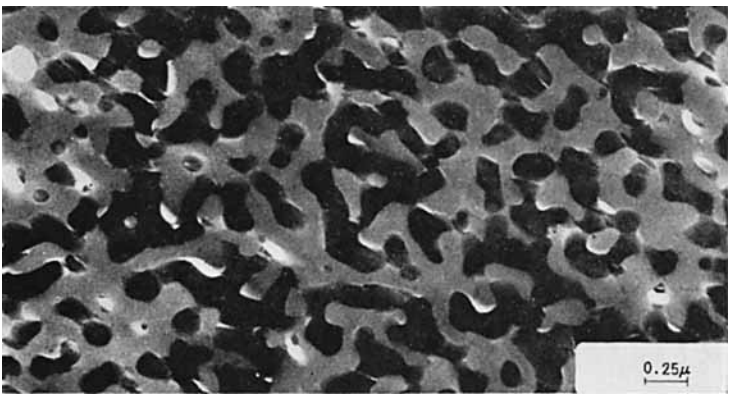

(3)

Figs. 2 and 3. Electron micrographs of porous glass CPG 10-1250. Magnification 40,000×.

CPG 10-1250 (Figs. 2 and 3). Unlike the CPG 10-2000 sample, this material appears to be a mixture of two pore size distributions, 1500 Å and 800 Å, with some voids up to 5000 Å readily apparent. At least 50% of this sample consists of solid glass. The average pore diameters, weighting Figures 2 and 3 equally on 150 measurements, is 1100 Å.

CPG 10-700 (Figs. 4 and 5). This material appears to have a broad pore size distribution averaging to a mean of 750 Å diameter, with some areas having diameters up to 4000 Å and some <50 Å. Many chips (Fig. 5) show large void diameters of ~2500 Å. Although some of the large voids may be due to glass dropout from the thin section (white holes), other large voids are free of holes.

CPG 10-370 (Fig. 6). The pore diameters of this and the CPG 10-240 sample are too small to measure with any degree of precision on the electron micrographs. In general overview, the sample contained about 5% voids with diameters of 1400 Å. These are *not* due to thin-section flaws. These

large voids in many cases are interconnected and may form channels throughout the chip.

CPG 10-240 (Figs. 7 and 8). This sample contains large sections free of voids and of very uniform pore diameter (Fig. 7). Some sections are filled with voids of 800 to 1200 Å diameter (Fig. 8).

The electron micrographs of the Corning porous glass are very similar to those seen previously with Bio-Rad laboratory glass.[6] The following items

(4)

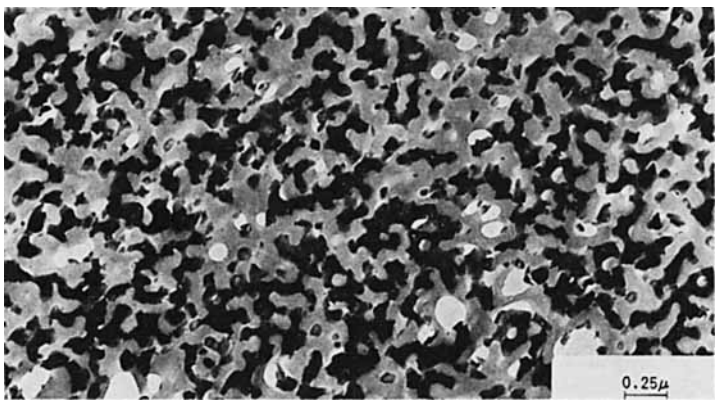

(5)

Figs. 4 and 5. Electron micrographs of porous glass CPG 10-700. Magnification 40,000×.

are notable exceptions: The pore diameter of the CPG 10-2000 sample is very uniform. The void density is very low in some chips of the smaller pore diameter glass. In general, the void volume of the glass appears to be lower in the Corning glass than in the Bio-Glas material. Some effort appears to have been made to reduce the solid glass wall volume in the Corning glass. The micrographs do not support the very narrow range of pore sizes present in each glass claimed by the manufacturer.

Mercury Porosimetry

The differential pore volume distributions determined by this method are shown in Figure 9. The results for the average radius determined from the maximum in the differential pore volume distribution are in general higher than the manufacturer's quoted values. Tangents to the differential pore volume were drawn, and the point where these lines intersected the

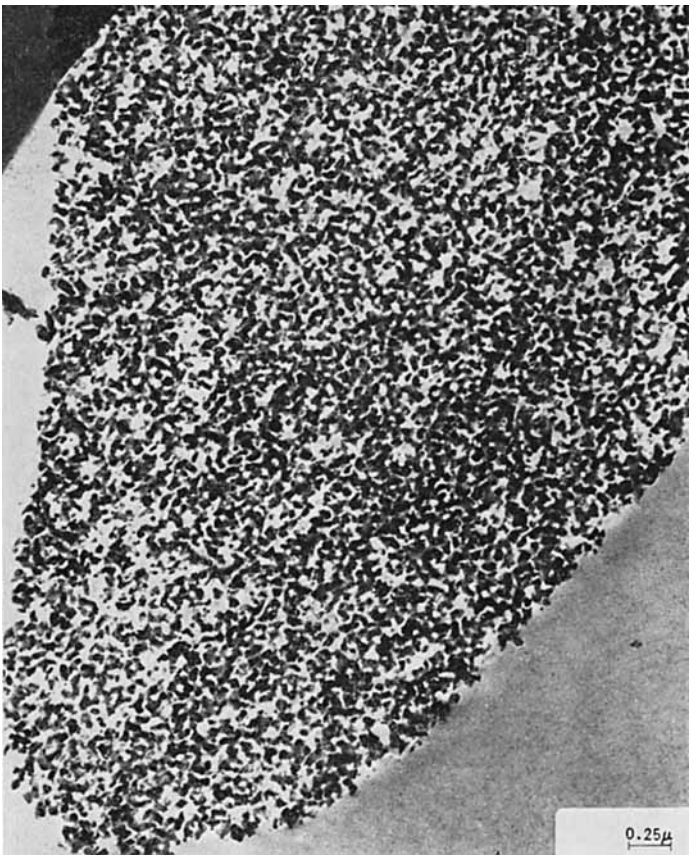

Fig. 6.

baseline were recorded to indicate the breadth of the pore size distribution. The cumulative pore volumes at which these pore radii occur are also shown in parentheses in Table I. In general, the smallest pores present in each sample quoted by the manufacturer are quite similar to the smallest pores present, as determined here by mercury porosimetry. The largest pores in each sample are considerably higher than the quoted values, and thus we find a considerably larger pore size distribution.

Nitrogen Adsorption–Desorption Isotherms

The first two samples of Table I have pore radii less than 500 Å and are thus amenable to analysis by this technique. The differential pore volume distributions determined from the desorption isotherms are shown for CPG 10-240 and CPG 10-370 in Figure 10. The CPG 10-370 shows a bimodal

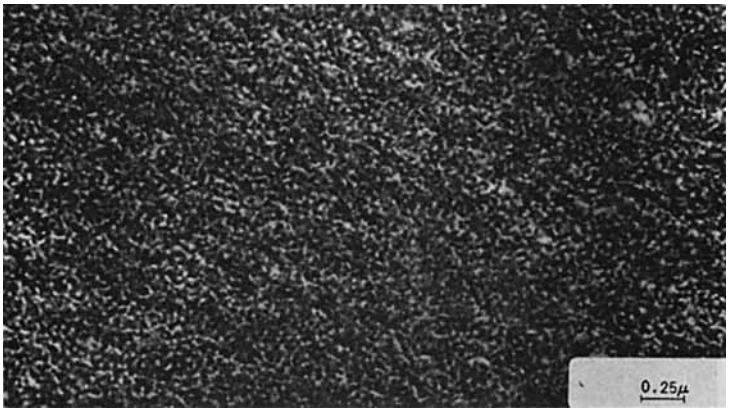

(7)

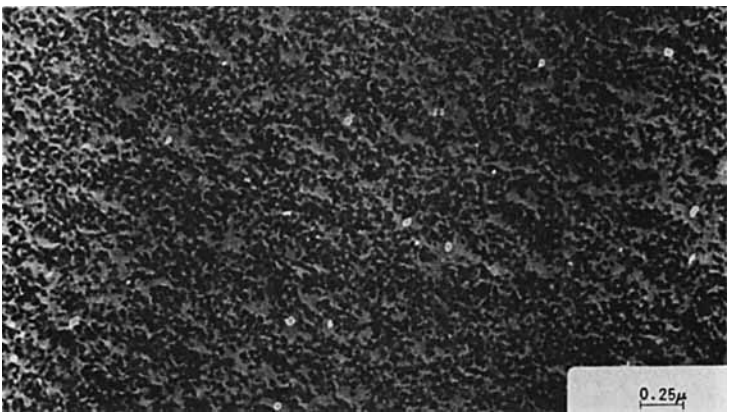

(8)

Figs. 7 and 8. Electron micrographs of porous glass CPG 10-240. Magnification 40,000×.

distribution. The values for the average pore radius from the maximum in the differential pore volume distribution are larger than both the manufacturer's quoted values and those determined here by mercury porosimetry.

The surface areas and pore volumes of these materials are shown in Table II. The volume of nitrogen adsorbed at a relative pressure of 0.98 measures the volume of pores having pore radii below 500 Å. The volume of mercury required to fill the pores is also recorded; this is also divided at a pore

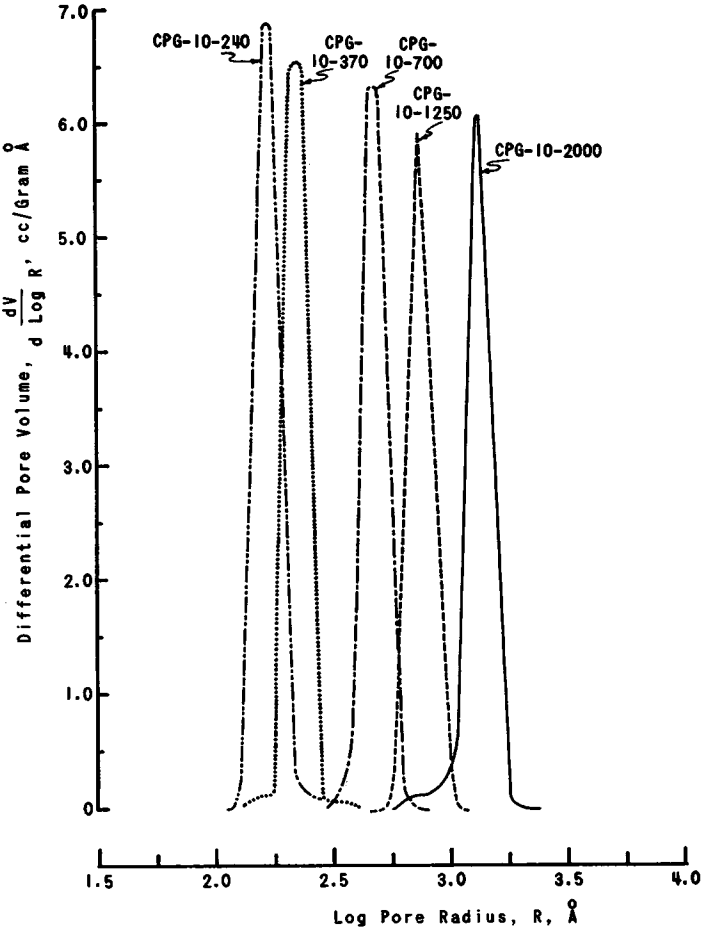

Fig. 9. Pore volume distribution of Corning porous glasses determined by mercury porosimetry.

radius of 500 Å to give a mercury macropore volume and a mercury micropore volume. In general, the values obtained here are considerably higher than the manufacturer's values. The agreement between the mercury micropore volume and the liquid nitrogen micropore volume is within 4%.

Gel Permeation Chromatography

The elution volume–molecular weight relationships are shown in Figure 11, plotted in the usual manner as the logarithm of the weight-average molecular weight versus elution volume in milliliters. From this figure, the effective separating range of each glass may be determined. None of the glasses is useful in the molecular weight range below 5000. The upper useful separating limits are as follows: CPG 10-240, 200,000; CPG 10-370, 400,000; CPG 10-700, 1.0×10^6; CPG 10-1250, 1.8×10^6; and CPG 10-

TABLE II
Pore Volumes and Surface Areas of Corning Porous Glass

Sample designation	Manufacturer's values pore volume, cc/g	BET surface area, m^2/g	Liquid nitrogen micropore volume,[a] cc/g	Mercury pore volume, cc/g		
				Total	Mercury micropore volume[b]	Mercury macropore volume[c]
CPG 10-240 Lot No. 8282P	0.72	70.0	0.95	0.99	0.99	0.0
CPG 10-370 Lot No. 8261P	0.80	53.6	0.84	0.86	0.86	0.0
CPG 10-700				0.90	0.58	0.32
Lot No. 8264S	0.78	21.7		0.88	0.65	0.23
CPG 10-1250				0.84	0.03	0.81
Lot No. 8255	0.76	10.6		0.87	0.06	0.81
CPG 10-2000 Lot No. 8154	0.85	7.3		0.88	0.04	0.84

[a] Pore volume having pore radii below 500 Å.
[b] Pore volume having pore radii between 22 and 500 Å.
[c] Pore volume having pore radii between 500 and 5020 Å.

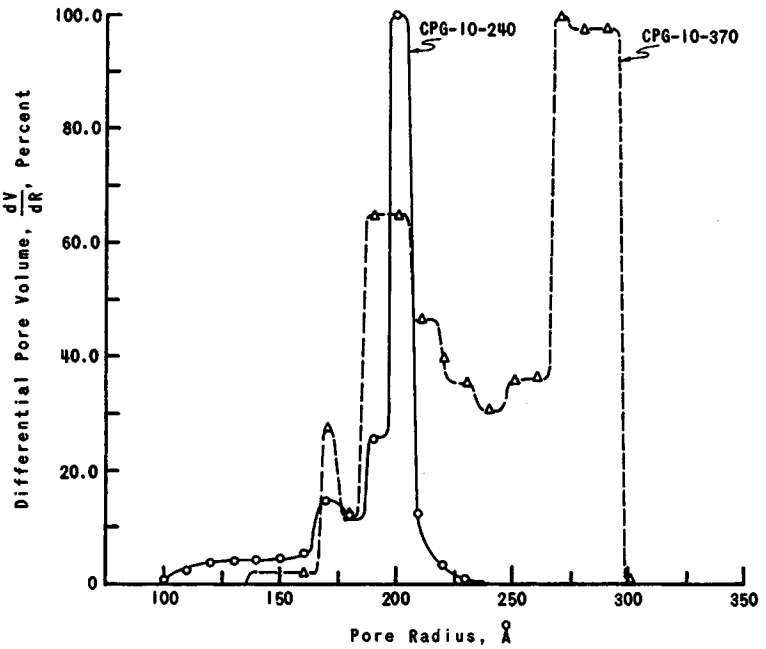

Fig. 10. Differential pore volume distribution of Corning porous glasses determined from nitrogen desorption isotherms.

TABLE III
GPC Elution Volumes and the Number of Theoretical Plates for Polystyrenes
Eluted from Corning Glass Columns Using Toluene at 25°C

Polystyrene molecular weight	Elution volume, V_e, ml					Theoretical plates/ft, n				
	CPG 10–240	CPG 10-370	CPG 10-700	CPG 10-1250	CPG 10-2000	CPG 10-240	CPG 10-370	CPG 10-700	CPG 10-1250	CPG 10-2000
1.8×10^6	26.24	27.51	26.84	26.88	35.39	112.3	121.0	43.0	18.1	8.4
860,000	26.37	27.68	28.53	33.48	39.58	117.4	129.0	30.0	20.3	15.0
670,000	26.46	27.85	29.88	35.05	41.14	118.1	118.0	25.4	20.4	15.1
411,000	26.58	28.45	33.69	38.56	42.92	101.0	99.0	24.7	24.3	19.8
160,000	29.21	33.44	39.87	42.84	45.46	64.4	59.5	31.0	34.0	22.9
97,200	32.93	37.25	42.54	44.40	46.56	60.5	70.2	32.9	40.9	25.6
51,000	38.23	41.48	44.79	46.06	47.62	60.1	79.4	34.3	46.7	29.3
19,800	43.90	45.38	46.99	47.37	48.26	82.0	104.5	41.5	55.7	31.5
10,300	46.22	47.11	47.84	47.75	48.64	96.8	116.5	43.4	58.0	34.9
4,000	48.26	48.38	48.43	48.21		114.6	159.0	44.8	65.8	
2,030	48.89	48.76		48.30	48.98	122.2	167.5		68.0	39.5
900	49.10	48.98	48.72	48.34	49.15	123.2	171.0	50.2	71.8	39.5
600		49.23	48.76	48.38	49.31		196.0	53.2	77.7	46.0
ODCB[a]	50.29	49.78	49.10	48.59	49.53	172.4	245.0	69.8	104	65.6
ODCB[b]	49.57	49.10	48.51	48.38	48.68	167.4	256.0	67.8	106	66.0

[a] Regular injection.
[b] Two-sec injection of a 6% by weight solution.

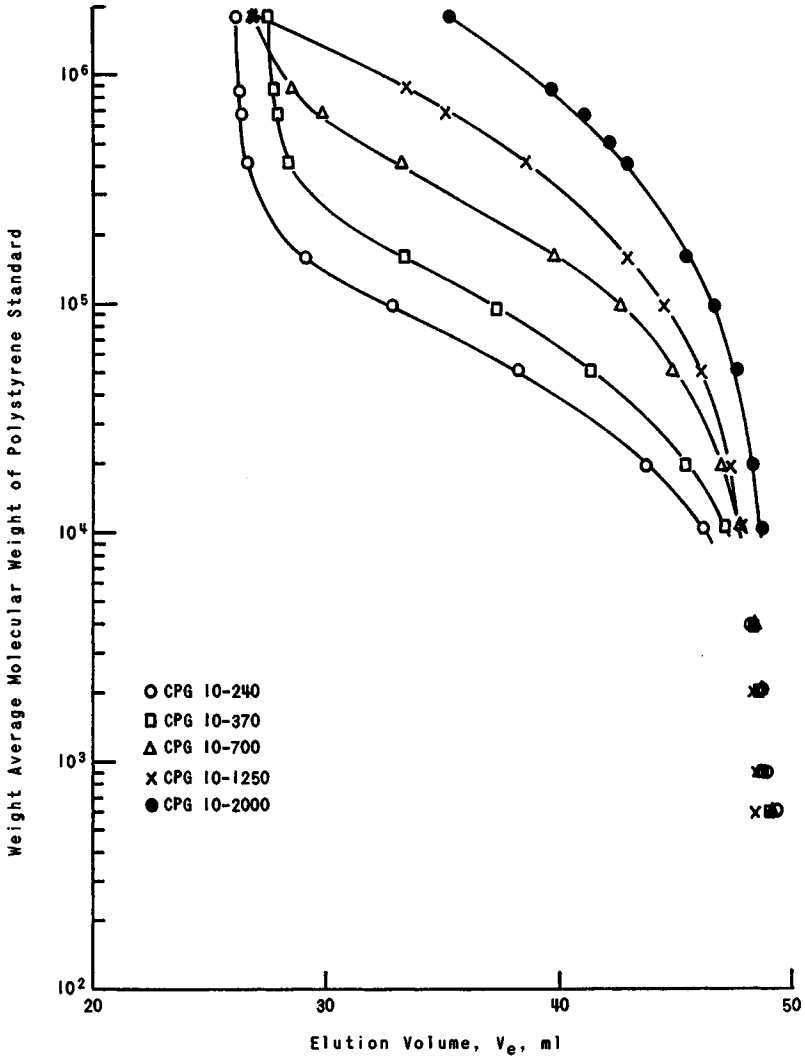

Fig. 11. Molecular weight elution curves for each column individually (O) CPG 10-240; (□) CPG 10-370; (Δ) CPG 10-700; (×) CPG 10-1250; (●) CPG 10-2000.

2000, $>2.0\times10^6$. The first three members of this series of glasses exhibit sigmoidal shapes generally found for GPC calibration curves. The linear parts of these relationships are fairly parallel. The glass CPG 10-1250 does not exhibit this shape but is convex to the elution volume axis. The packing with the largest pores, CPG 10-2000, could not be fully evaluated with the presently available standards. As the pore volumes of these materials are all approximately the same, the void volume of the largest pore diameter packing column would be expected to be 26 or 27 ml. As the 1.8×10^6 molecular weight polystyrene elutes at 35.39 ml, the exclusion limit of this

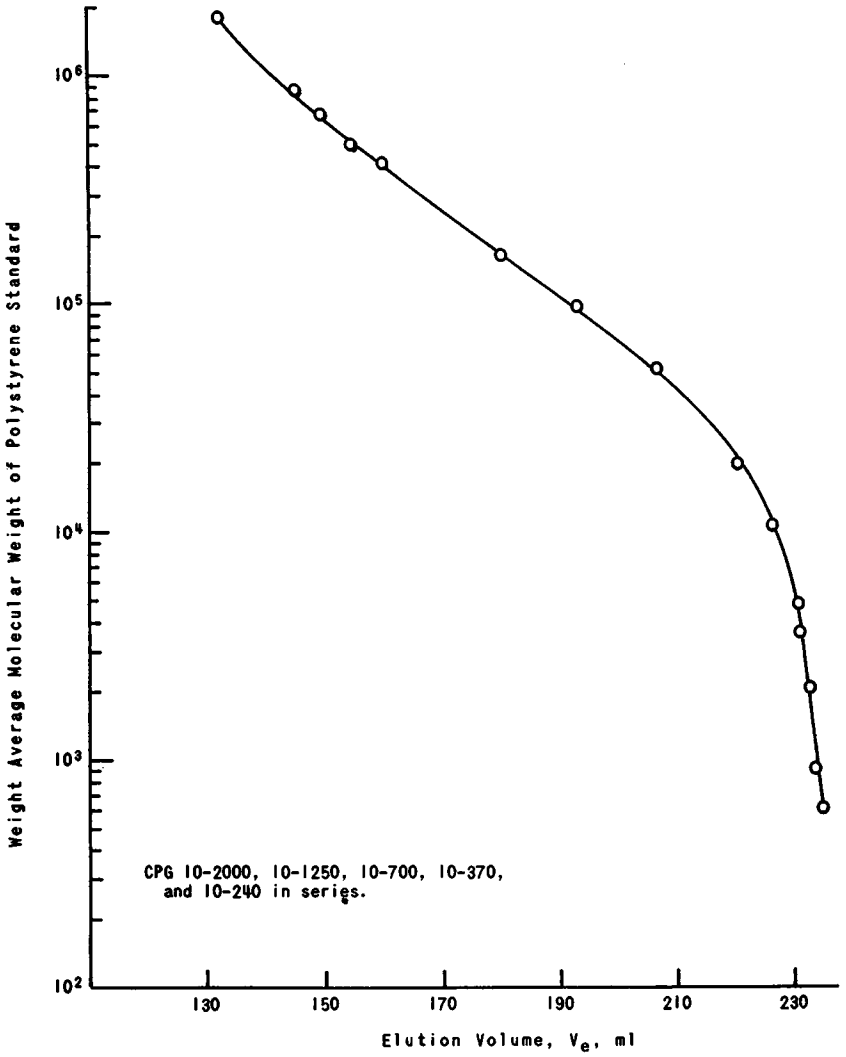

Fig. 12. Molecular weight elution curve with all columns in series.

column should be considerably higher than 1.8×10^6. The calibration curve for these five columns connected in series is shown in Figure 12.

In Table III are shown elution volumes and the efficiencies of these columns expressed as the number of theoretical plates per foot, n, calculated from

$$n = \frac{1}{L}\left[\frac{V_e}{0.25w_b}\right]^2 \tag{1}$$

where L = the column length, in ft; V_e = the elution volume, in ml; and w_b = the width of the peak where the tangents at the points of inflection intersect the baseline, in ml.

Because these packing materials have a larger pore volume than other glasses available, the separation between the void volume V_0 and the total liquid volume V_e of the column is considerably increased. The efficiencies of the columns show considerable variations, considering that the columns were all packed in a similar fashion. The efficiencies of these columns do not vary in any systematic manner with pore volume, pore radius, or the elution volume of the *o*-dichlorobenzene solute.

For each column, the efficiency drops as the molecular weight increases. This continues to decrease as long as the solutes are not eluting at the void volume. When this happens, the efficiencies increase again because no band broadening due to the pore permeation process or the finite molecular weight distribution is present. Where several species elute at the void volume, their efficiencies are all fairly similar for a given column.

The pore volume calculated from the physical characterizations of the packings and the weight of packing in each column agree with the difference between the total volume and void volume of the column within 5% (Table IV). The CPG 10-2000 data are not complete inasmuch as the void volume

TABLE IV
Comparison of Calculated and Experimental Pore Volumes of Corning Porous Glass Columns

Porous glass	Wt. of packing in column, g	Pore volume, ml/g	Pore volume in column, ml	$V_t - V_0$, ml	Theoretical plates/ft for *o*-dichlorobenzene, n
CPG 10-240	25.3	0.99	25.3	24.05	172.4
CPG 10-370	26.2	0.86	22.5	22.3	245.0
CPG 10-700	27.9	0.89	24.8	22.3	69.8
CPG 10-1250	29.0	0.855	24.8	21.7	104
CPG 10-2000	26.3	0.88	—	—	65.6

was not experimentally determined. The elution volumes determined on the series combination are in excellent agreement with the additive values for the individual columns when allowance is made for the fact that the injection loop volume is included four additional times for the individual column total and the fact that a small volume is added to the series combination because of the tubing used to connect the columns. The number of theoretical plates for the series combination is calculated from the individual column values by use of eqs. (1) and (2):[7]

$$n_{TOT} = \frac{1}{\Sigma L}\left|\frac{(\Sigma V_e)^2}{\Sigma(w_b/4)^2}\right| = \frac{1}{\Sigma L}\left|\frac{\Sigma(V_e)^2}{\Sigma(V_e^2/n)}\right|. \quad (2)$$

Again, excellent agreement is found (Table V) between the observed and calculated values. If the number of columns, x, of equal length are con-

TABLE V
Elution Volumes and Number of Theoretical Plates
of Polystyrene Solutes Eluted from Corning Porous Glass Columns

Polystyrene molecular weight	Elution volume for series combination, ml	Theoretical plates/ft for series combination	Calculated elution volume[a] from each column, ml	Calculated theoretical plates/ft[b] from each column
1.8×10^6	132.20	12.55	131.90	12.48
860,000	145.53	19.20	144.73	19.03
670,000	149.55	19.45	149.47	19.44
498,000	154.80	21.90		
411,000	160.01	25.80	159.29	25.61
160,000	180.37	30.80	179.91	30.70
97,200	193.07	37.90	192.77	37.70
51,000	206.82	40.40	207.30	40.53
19,800	220.45	47.50	220.99	47.49
10,300	226.04	53.50	226.65	53.96
4,000				
2,030	232.94	69.5		
900	233.20	73.0	233.38	72.95
600	234.34	80.3	234.42	80.56
ODCB[c]	235.78	113.5	236.38	114.48
ODCB[d]	234.68	117.0	233.33	114.77

[a] Sum of individual values, see text.
[b] Calculated from eq. (1).
[c] Regular injection.
[d] Two-sec injection of a 6% by weight solution.

nected in series and the elution volumes of the solute being used to determine the plate count are similar for each column, then eq. (2) simplifies to

$$n_{TOT} = \frac{x}{\Sigma\left(\frac{1}{n_i}\right)}. \tag{3}$$

This equation could not be used here because of considerable differences in elution volume for the various columns at constant solute molecular weight. The peak widths w_b, in ml, are tabulated in Table VI for each of the five columns run individually. Also included in this table are the peak widths calculated for a series combination by use of the summation $[\Sigma(w_b)^2]^{1/2}$ and the experimentally determined peak width for the series combination of the five columns. The experimental values are quite close to the calculated values, being somewhat larger at high molecular weights and smaller for the smaller molecules. The values of the peak widths due to the passage through the column interstices and the pores, if the molecule is not totally excluded, W_{GPC}, are shown in Table VII. These were calculated from the following equation:

$$W_{TOT}^2 = W_{MWD}^2 + W_{INST}^2 + W_{GPC}^2 \tag{4}$$

TABLE VI
Peak Widths of Polystyrene Solutes Eluted from Corning Porous Glass Columns

Polystyrene molecular weight	Peak width at the base, w_b, ml					$[\Sigma(w_b)^2]^{1/2}$ for CPG 10-240, 10-370, 10-700, 10-1250, 10-2000 individually, ml	w_b for CPG 10-240, from 10-370, 10-700, 10-1250, 10-2000 in series combination, ml
	CPG 10-240	CPG 10-370	CPG 10-700	CPG 10-1250	CPG 10-2000		
1.8×10^6	4.95	4.99	12.61	8.17	24.42	29.52	33.40
860,000	4.87	4.87	14.90	10.41	20.32	28.04	29.68
670,000	4.87	5.16	15.49	11.85	21.17	29.20	30.32
498,000	—	—	—	—	19.81	—	—
411,000	5.29	5.71	15.66	13.55	19.18		28.16
160,000	7.29	8.68	14.69	14.31	19.01	30.12	29.04
97,000	8.47	8.89	13.88	14.82	18.41	29.96	28.08
51,000	9.86	9.31	13.46	15.28	17.61	30.12	29.14
19,800	9.69	8.89	12.70	14.56	17.23	29.00	28.68
10,300	9.40	8.72	12.53	14.56	16.42	28.32	27.60
4,800	—	—	—	—	16.09	—	25.48
4,000	9.02	7.70	11.89	14.48	—	—	—
3,600	—	—	—	—	16.09	—	25.80
2,030	8.85	7.53	11.73	—	15.58	—	25.04
900	8.89	7.49	11.43	13.76	15.66	26.44	24.44
600	8.47	7.02	11.01	13.38	14.52	25.12	23.36
o-Dichlorobenzene[a]	7.66	6.35	9.52	11.77	12.23	21.96	19.76
o-Dichlorobenzene[b]	7.53	6.14	9.40	11.77	11.98	21.52	19.48

[a] Regular injection.
[b] Two-sec injection of a 6% by weight solution.

TABLE VII
Peak Widths of Polystyrene Standards Eluted from Corning Glass Columns Correct for Instrumental Broadening and the Finite Molecular Weight Distribution of the Polymer

$\bar{M}_w$	$\bar{M}_w/\bar{M}_n$	W_{TOT}	W_{MWD}	W_{INST}	W_{GPC}
860,000	1.15	29.68	25	3.1	15.69
670,000	1.2	30.32	25.0	3.1	16.87
411,000	1.06	28.16	18.0	3.1	21.43
160,000	1.06	29.04	18.0	3.1	22.57
97,200	1.06	28.08	17.0	3.1	22.13
51,000	1.06	29.12	16.5	3.1	23.79
19,800	1.06	28.68	9.0	3.1	27.05
10,300	1.06	27.60	5.5	3.1	26.87
4,800	1.1	25.48	3.5	3.1	25.04
3,600	1.1	25.80	2.5	3.1	25.49
2,030	1.1	25.04	2.0	3.1	24.77
900	1.1	24.44	1.5	3.1	24.20
600	1.1	23.36	1.0	3.1	23.13
o-Dichlorobenzene		19.76	0	2.68	19.58

where W_{TOT}, W_{MWD}, and W_{INST} represent the total peak width, the peak width due to molecular weight distribution, and the instrumental (non-column) spreading, respectively. W_{MWD} was calculated on the assumption that the polymers studied could be represented by a log normal distribution. The molecular weight limits were set at 5 and 95 wt-% composition of the polymer. For each polymer, the elution volume between these two molecular weight limits was determined from the calibration curve.

The instrumental spreading was determined by removing the column and joining up the connecting tubing. As may be seen from Table VII, the values of the total peak width W_{TOT} increase fairly regularly with molecular weight. However, when the total peak width is corrected for instrumental spreading, W_{INST}, and the finite molecular weight range in each sample, W_{MWD}, the values of the peak width due to the chromatographic process, W_{GPC}, do not increase in this regular manner. The peak widths actually show a decrease as the molecular weight is increased. The observed trend does not agree with previous results,[8,9,10] which report the dependence of the efficiency of the GPC process on the diffusion coefficient of the solute molecules, i.e., peak width increasing with increasing molecular weight. This result had previously been found not to be valid for GPC using a polystyrene gel column[11] and a broad pore size distribution glass column.[1]

CONCLUSIONS

The porous glasses studied have been shown to be effective substrates for GPC separations. The very large pore volume compared with other available packing materials is a real advantage, resulting in a better separation between different solutes for the same-sized column. The pore size distribution of the lot of porous glass studied in this paper has been found to be

broader than specified by the manufacturer, and these materials should not be used for testing theoretical relationships in GPC requiring the use of a very narrow pore size distribution material. The elution volume for a series combination of the individual columns was shown to be additive, and the peak widths were additive as the squares of the peak widths for the individual columns. The efficiencies of these columns were comparable to those of other available glass packings. The observed peak widths, corrected for instrumental spreading and the finite molecular weight distribution of the solutes, decreased with increasing molecular weight, indicating little dependence of efficiency on the diffusion coefficient.

References

1. A. R. Cooper, A. R. Bruzzone, J. H. Cain, E. M. Barrall, II, and J. F. Johnson, *Separation Science*, in press.
2. M. J. R. Cantow and J. F. Johnson, *J. Appl. Polym. Sci.*, **11**, 1851 (1967).
3. W. J. Haller, *J. Chem. Phys.*, **42**, 686 (1965).
4. W. J. Haller, *Nature*, **206**, 693 (1965).
5. J. C. Moore and M. C. Arrington, *Preprints of 3rd International Seminar on Gel Permeation Chromatography*, Geneva, May 1966.
6. E. M. Barrall and J. H. Cain, *J. Polym. Sci.*, **C21**, 253 (1968).
7. J. Kwok, L. R. Snyder, and J. C. Sternberg, *Anal. Chem.*, **40**, 118 (1968).
8. M. LePage and A. J. DeVries, *3rd International Seminar on Gel Permeation Chromatography Preprints*, Geneva, May 1966.
9. W. B. Smith and A. Kollmansberger, *J. Phys. Chem.*, **69**, 1457 (1965).
10. J. G. Hendrickson, *J. Polym. Sci. A-2*, **6**, 1903 (1968).
11. A. R. Cooper, A. R. Bruzzone, and J. F. Johnson, *Amer. Chem. Soc. Polymer Preprints*, **10**, 1455 (1969).

Received October 22, 1970
Revised November 19, 1970